

Enhanced photocurrent efficiency of a carbon nanotube p–n junction electromagnetically coupled to a photonic structure

Bryan M Wong and Alfredo M Morales

Materials Chemistry Department, Sandia National Laboratories, Livermore, CA 94551, USA

E-mail: bmwong@sandia.gov

Received 5 November 2008, in final form 17 January 2009

Published 19 February 2009

Online at stacks.iop.org/JPhysD/42/055111

Abstract

We present photocurrent power-enhancement calculations of a carbon nanotube p–n junction electromagnetically coupled to a highly efficient photonic structure. Particular attention is paid to a GaAs photonic structure specifically modified to increase the intensity of infrared light onto the nanotube region for effective energy conversion. Using finite-difference time-domain calculations, we compute a significant increase in electric field intensity in the nanotube region which enables an estimation of power efficiency. These results demonstrate the potential of using a photonic structure to couple large-scale infrared sources with carbon nanotubes while still retaining all the unique optoelectronic properties found at the nanoscale.

(Some figures in this article are in colour only in the electronic version)

1. Introduction

One of the most rapidly growing areas in nanoscience is the ability to artificially manipulate optical and electrical properties at the nanoscale. In particular, nanomaterials such as single-wall carbon nanotubes can convert incident light into photocurrent due to their unique one-dimensional electronic properties [1]. Indeed, recent experimental measurements have shown that a single carbon nanotube can act as a polarized photodetector with quantum efficiencies greater than 10% [2]. In addition to intrinsic optoelectronic efficiency, carbon nanotubes exhibit ballistic charge transport at room temperature [3], potentially enabling high-performance photodetectors that need not be cryogenically cooled.

While numerous theoretical and experimental studies have been carried out to exploit the electronic properties of individual carbon nanotubes, it has been difficult to efficiently couple microscale technologies to their nanoscale properties. In particular, one of the most limiting factors in making nanotube-based photodetectors a viable technology is their relatively small absorption cross-section. Since the diameter of a nanotube is of the order of 1 nm, its light-collecting surface

area is limited to this small length scale, and radiation which is not directly incident on the nanotube will go undetected [4, 5].

To address this problem, we investigate the photocurrent efficiency of a carbon nanotube p–n junction when it is illuminated by a highly efficient photonic structure. This coupling of carbon nanotubes with photonic structures is a natural and logical step towards bridging microscale and nanoscale length scales. By artificially modifying the composition and periodic arrangement in a photonic structure, the flow of light can be guided onto extremely localized regions of space. Recognizing these possibilities, several groups have already characterized photonic structures which can focus electromagnetic waves and provide highly directional light beams [6–14]. There has also been recent work in modifying photonic surfaces to produce beams with high transmission efficiencies [8]. In this work, we specifically calculate the efficiency of a carbon nanotube p–n junction which is electromagnetically coupled to a planar GaAs photonic structure. To validate the performance of the photonic system, finite-difference time-domain (FDTD) calculations are used to calculate electric field enhancements, power intensities and coupling efficiencies. The resulting FDTD calculations enable

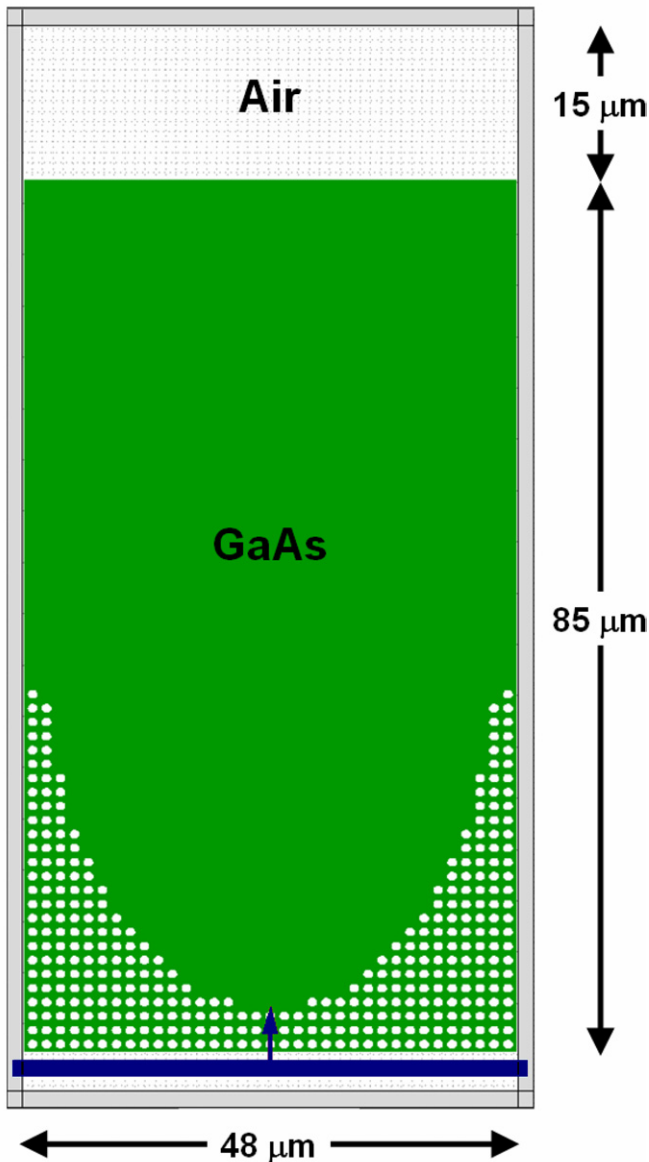


Figure 1. GaAs photonic structure enclosed by absorbing boundary layers with $15 \mu\text{m}$ of air between the top boundary and the cleaved GaAs slab. The ratio of the air hole radius to the lattice spacing is $r/a = 0.3$, where $a = 1.365 \mu\text{m}$. A plane wave approaching the structure from below is depicted by an upward-pointing arrow.

an estimation of nanotube photocurrent efficiency within the linear response regime and also provide guidance on enhancing this efficiency using a photonic structure.

2. Photonic structure specifications

For the nanotube-photonic structure in this work, we are primarily interested in the infrared region of the electromagnetic spectrum. In order to make an efficient photodetector in this region of light, one must be careful in choosing a wavelength which is not coincident with a strong water absorption peak. In addition, since we are also interested in future experimental studies on our structure, one must choose a wavelength which can be easily produced by a conventional CO_2 laser source. For these two reasons, we have

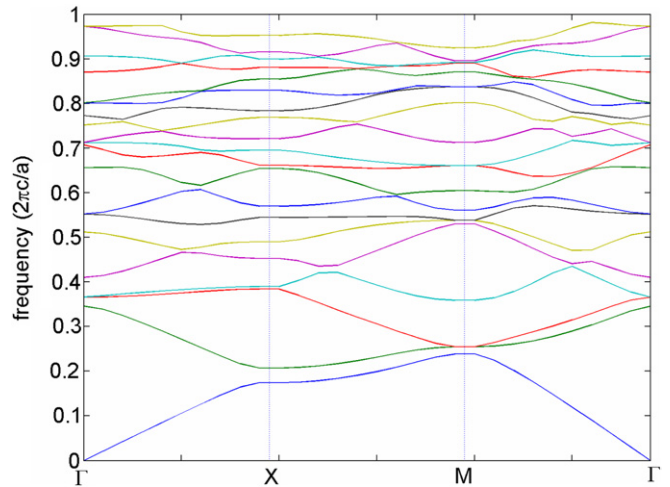


Figure 2. Calculated photonic band structure of the GaAs photonic array. A wavelength of $10.6 \mu\text{m}$ lies in a frequency range contained in the first band for incident light along any direction.

chosen a wavelength of $10.6 \mu\text{m}$ to perform all of our FDTD simulations and numerical analysis. The two-dimensional photonic structure considered in this work is based on the design of Lin *et al* [12] who originally used a silicon structure to couple terahertz radiation into a narrow waveguide. In order to function efficiently with our chosen wavelength of $10.6 \mu\text{m}$, a few modifications have been made to their original design. The most significant and important modification is the use of a GaAs ($\epsilon = 13.2$) photonic substrate which is largely transparent to infrared light [15]. The photonic structure studied here is a periodic square array of air holes arranged on a $48 \mu\text{m} \times 85 \mu\text{m}$ GaAs slab shown in figure 1. The entire photonic structure is enclosed by absorbing boundary layers with $15 \mu\text{m}$ of air ($\epsilon = 1.0$) between the top boundary layer and the cleaved GaAs slab. The ratio of the air hole radius to the lattice spacing is $r/a = 0.3$, where $a = 1.365 \mu\text{m}$. The corresponding band structure of this periodic array is shown in figure 2 for all wave vectors along the edges of the irreducible Brillouin zone defined by the points Γ , M and X . Using a plane-wave expansion method [16], the resulting band structure was obtained for a transverse magnetic (TM) mode which has its electric field perpendicular to the plane of the GaAs slab (cf figure 3). For both the plane-wave and FDTD simulations, an effective index of 3.0 was used for the background GaAs material. From the band structure, it can be deduced that a wavelength of $10.6 \mu\text{m}$ lies in a frequency range contained in the first band for incident light along any direction. By choosing the incident light to coincide with a frequency in the first band, any plane wave launched into the photonic structure will propagate with minimal transmission loss. Once the light has been guided through the photonic surface, the propagation path of the incident plane wave will be bent and altered by the pattern of air holes in the GaAs substrate.

To investigate the focusing effects of the photonic structure, a two-dimensional FDTD method was used to propagate Maxwell's equations in time and space throughout the entire structure [13]. A $50 \mu\text{m}$ wide input wave

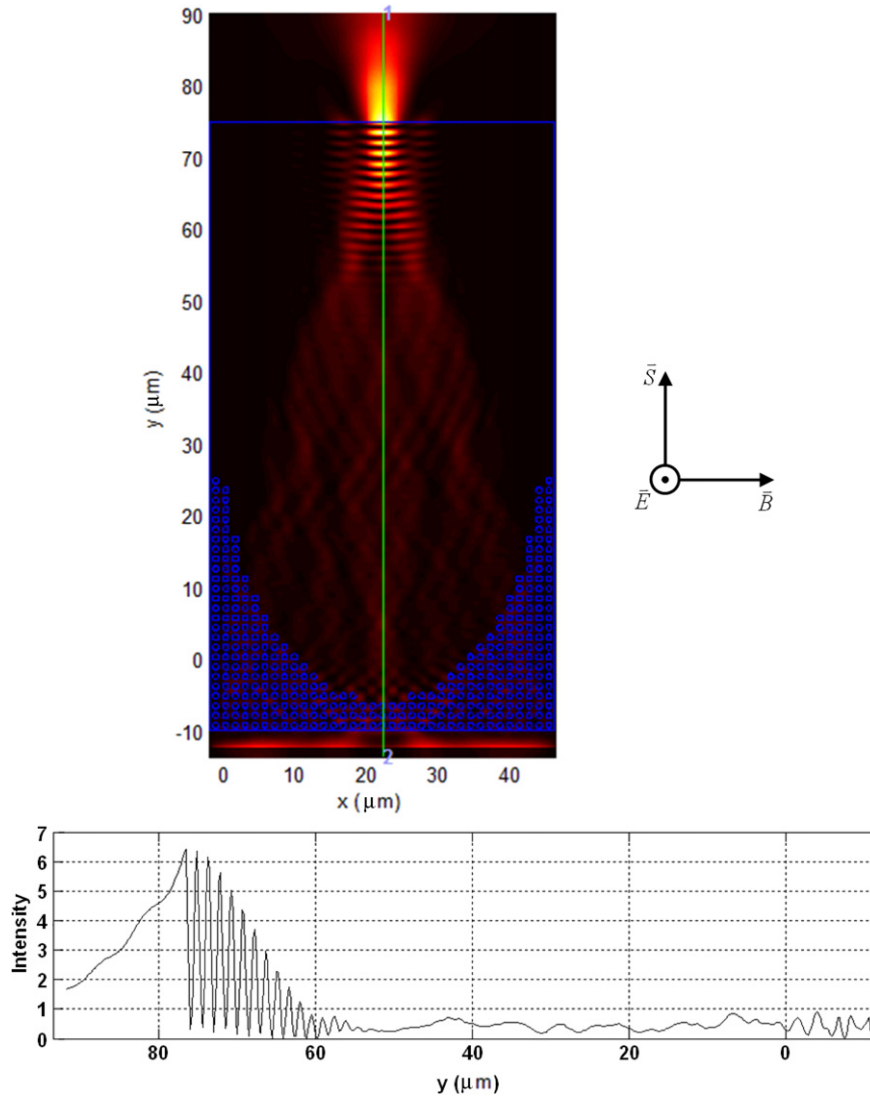


Figure 3. Intensity profile of the GaAs photonic structure obtained from a two-dimensional FDTD analysis. The orientations of the electric (\vec{E}), magnetic (\vec{B}) and Poynting (\vec{S}) vectors are shown on the right. The z -component of the electric field intensity along the vertical line drawn on the GaAs photonic structure is plotted below. The source intensity is normalized to a value of 1.0.

(10.6 μm wavelength) was launched along the ΓX direction into the photonic structure, and the steady-state electric field intensities ($\propto |E_z|^2$) are shown in figure 3. After passing through the array of air holes, the light propagates over several micrometres, subsequently focuses and finally exits the GaAs material into air. The performance of the photonic structure can be quantitatively characterized by calculating the E_z intensity along a vertical line through the centre of the structure. As shown in figure 3, the photonic structure tightly focuses the wide plane wave into a narrow 5 μm wide region which lies 0.1 μm outside the cleaved GaAs facet. Along this line scan, the electric field intensity reaches a maximum value of 6.25 relative to the source intensity which was set to a value of 1.0. It is also interesting to note that an uncleaved GaAs slab without the 15 μm air interface yields an intensity which is reduced by a factor of 2.5 compared with the present photonic structure. The increased intensity of the present configuration is mostly due to the rapid change in permittivity as the light waves approach the GaAs–air interface. Once the light finally

exits the GaAs material into air, it slightly refocuses near the interface again before spreading out into free space. In order to assess the efficiency of our photonic structure, we calculated the magnitude of the Poynting vector ($\vec{S} = 1/\mu_0 \vec{E} \times \vec{B}$) as a function of position with the GaAs slab. From the E_z and B_x field distributions, a coupling efficiency of 63% was obtained by integrating the y -component of the Poynting vector across a 10 μm wide region near the focusing point and dividing it by a similar integration across the entire 50 μm source region. In other words, 63% of the input power due to the 50 μm -wide light wave is focused in a 10 μm wide region near the GaAs–air interface.

We also performed FDTD calculations on identical GaAs patterns with various air hole radii (r) and lattice spacing parameters (a) to investigate their effect on modulating the electric field intensity. Specifically, we chose the following five sets of configurations: $(r, a) = (r_0, a_0), (r_0 - 2 \mu\text{m}, a_0), (r_0 + 2 \mu\text{m}, a_0), (r_0, a_0 - 2 \mu\text{m})$ and $(r_0, a_0 + 2 \mu\text{m})$, where the $r_0 = 0.4095 \mu\text{m}$ and $a_0 = 1.365 \mu\text{m}$ values

Table 1. Maximum intensities and their positions for various air hole radii (r) and lattice spacing parameters (a). All calculations were performed with the same pattern depicted in figure 1 using an uncleaved GaAs slab, and intensities are reported relative to the source intensity which was normalized to a value of 1.0. The positions of maximum intensity are measured relative to the bottom of the GaAs photonic structure.

Air hole radius, r (μm)	Lattice spacing, a (μm)	Maximum relative intensity	Position of maximum intensity (μm)
0.210	1.365	1.18	145
0.410	1.165	3.20	60
0.410	1.365	2.00	85
0.410	1.565	0.24	25
0.610	1.365	3.20	55

correspond to the same parameters used in our original photonic structure described previously. All of these FDTD calculations were performed with the same pattern depicted in figure 1 using an uncleaved GaAs slab to make the analysis more straightforward. Table 1 compares the maximum intensities and their positions relative to the bottom of the structure for all five configurations. Based on our FDTD simulations, the results confirm the expected trend that one can increase the maximum intensity by increasing the air hole radius (r) and decreasing the lattice spacing (a). It is important to note, however, that one is ultimately limited by values of r and a which satisfy the constraint $r/a < 1/2$ (ratios larger than $1/2$ have overlapping air holes). Furthermore, increasing the r/a ratio to maximize electric field intensity will pose severe experimental difficulties as the GaAs substrate between adjacent air holes becomes thinner. Simultaneously maximizing intensity within the constraints of experimental fabrication methods is an interesting optimization problem which we are currently investigating.

3. Carbon nanotube photocurrent calculations

The final step in evaluating the efficiency of this nanotube-photonic device is to calculate the increase in nanotube photocurrent due to the photonic structure. As mentioned previously, a carbon nanotube acts as a polarized photodetector and generates maximal photocurrent when the incident radiation has its electric field parallel to the nanotube axis. Since the photonic structure is operating in the TM mode with the E_z component perpendicular to the plane of the GaAs slab, the carbon nanotube p–n junction was placed near the GaAs–air interface with its axis parallel to the E_z field for maximum efficiency. Figure 4 depicts in greater detail the orientation of the nanotube-photonic structure relative to the electric (\vec{E}), magnetic (\vec{B}) and Poynting (\vec{S}) vectors.

The theoretical performance of a nanotube p–n junction under bias has been described by Stewart and Leonard [17]. Their calculation was based on an idealized (17, 0) zigzag nanotube p–n junction which can be selectively doped to absorb in the infrared region. Further details on the dopant concentrations and their nanotube p–n junction model can be found in [18]. Using a self-consistent nonequilibrium Green’s

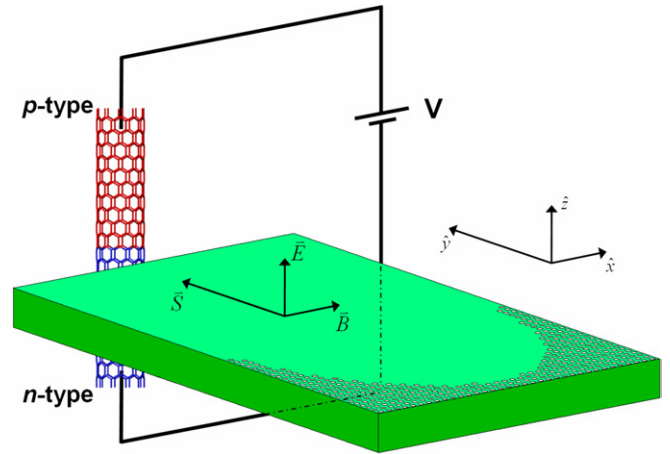


Figure 4. Schematic of a carbon nanotube p–n junction (not drawn to scale) electromagnetically coupled to the GaAs photonic structure. The nanotube p–n junction is placed under an external bias voltage, V . The outgoing radiation from the photonic structure has its electric field parallel to the nanotube axis and a Poynting vector perpendicular to the nanotube surface.

function approach, Stewart and Leonard calculated current–voltage characteristics of illuminated carbon nanotubes under an applied voltage bias. Under low power conditions, one can use their expression for the efficiency η of a nanotube p–n junction under bias given by [17]

$$\eta = \frac{kT}{4eI_s} \frac{I_{\text{ph}}^2}{P_{\text{op}}}, \quad (1)$$

where I_s is the saturation current of the nanotube, I_{ph} is the current generated by the electron–photon interaction and P_{op} is the optical power delivered to the nanotube. Since I_{ph} depends linearly on P_{op} , equation (1) reduces to $\eta \propto P_{\text{op}}$ in the low optical power limit. Therefore, a relative intensity of 6.25 obtained from the FDTD calculations directly translates into a factor of $6.25 \times$ enhancement (or alternatively, a 525% increase) in photocurrent efficiency.

While we have specifically focused on a GaAs photonic slab structure, it is clear that merging these two technologies needs further study. To our knowledge, the experimental photocurrent of a carbon nanotube electromagnetically coupled to a photonic structure has not been tested and remains unknown. Experimental measurements on the photocurrent power efficiency combining these two technologies would be extremely valuable as a check on our theoretical calculations.

4. Conclusion

In conclusion, we have investigated the feasibility of using a photonic structure to enhance the photocurrent efficiency of a carbon nanotube device. Using a two-dimensional FDTD method, we designed a GaAs photonic structure which modulates the propagation of infrared light to focus plane waves into a $5 \mu\text{m}$ wide region. The subsequent increase in electric field intensity in this region enables the computation of power efficiency within the linear response regime.

Using a low-power approximation for the carbon nanotube junction response, the photonic structure thus designed enables a 525% increase in photocurrent. We are currently investigating other experimentally fabricable designs which can further increase the electromagnetic coupling to a nanotube p–n junction. Photonic structures may also be combined with other chemical methods which direct and control the electronic properties of the nanotubes themselves to further enhance the photocurrent efficiency. One promising method already under study is the noncovalent chemical functionalization of carbon nanotubes [19].

Acknowledgments

Supported by the Laboratory Directed Research and Development program at Sandia National Laboratory, a multiprogram laboratory operated by Sandia Corporation, a Lockheed Martin Company, for the United States Department of Energy's National Nuclear Security Administration under contract DE-AC04-94AL85000.

References

- [1] Saito R, Dresselhaus G and Dresselhaus M S 1998 *Physical Properties of Carbon Nanotubes* (London: Imperial College Press)
- [2] Freitag M, Martin Y, Misewich J A, Martel R and Avouris Ph 2003 *Nano Lett.* **3** 1067
- [3] Javey A, Guo J, Wang Q, Lundstrom M and Dai H 2003 *Nature* **424** 654
- [4] Burke P J, Li S and Yu Z 2006 *IEEE Trans. Nanotechnol.* **5** 314
- [5] Kempa K *et al* 2007 *Adv. Mater.* **19** 421
- [6] Ozbay E, Aydin K, Bulu I and Guven K 2007 *J. Phys. D: Appl. Phys.* **40** 2652
- [7] Li Z, Aydin K and Ozbay E 2008 *J. Phys. D: Appl. Phys.* **41** 155115
- [8] Wang Q, Cui Y, Yan C, Zhang L and Zhang J 2008 *J. Phys. D: Appl. Phys.* **41** 105110
- [9] Vodo P, Parimi P V, Lu W T and Sridhar S 2005 *Appl. Phys. Lett.* **86** 201108
- [10] Qiu M, Thylén L, Swillo M and Jaskorzynska B 2003 *IEEE J. Quantum Electron.* **9** 106
- [11] Berrier A, Mulot M, Swillo M, Qiu M, Thylén L, Talneau A and Anand S 2004 *Phys. Rev. Lett.* **93** 073902-1
- [12] Lin C, Chen C, Sharkawy A, Schneider G J, Venkataraman S and Prather D W 2005 *Opt. Lett.* **30** 1330
- [13] Sharkawy A, Pustai D, Shi S, Prather D W, McBride S and Zanzucchi P 2005 *Opt. Express* **13** 2814
- [14] Prather D W, Shi S, Murakowski J, Schneider G J, Sharkawy A, Chen C and Miao B 2006 *IEEE J. Quantum Electron.* **12** 1416
- [15] Brozel M R and Stillman G E 1996 *Properties of Gallium Arsenide* 3rd edn (London: Institution of Electrical Engineers)
- [16] Joannopoulos J, Mead R and Winn J 1995 *Photonic Crystals* (Princeton, NJ: Princeton University Press)
- [17] Stewart D A and Léonard F 2005 *Nano Lett.* **5**, 219
- [18] Léonard F and Tersoff J 2000 *Phys. Rev. Lett.* **85** 4767
- [19] Zhou X, Zifer T, Wong B M, Krafcik K L, Léonard F and Vance A L 2009 Color detection using chromophore-nanotube hybrid devices *Nano Lett.* at press doi:10.1021/nl8032922